ROCK FALL CASE STUDY: HAWKESBURY SANDSTONE

Daniel Bishop[1], Stephen Fityus[2], David Piccolo[3] and Garry Mostyn[3]
[1]Research Associate, University of Newcastle, [2]University of Newcastle, [3]Pells Sullivan Meynink.

ABSTRACT

This paper documents a rock fall in the Hawkesbury Sandstone. Two distinct phases, preceding the ultimate rock fall event have been identified and documented; a creep-loading phase and a rock fracture phase. Water is identified as playing a significant role in the creep-loading phase. Over the long term, peak water pressures from intermittent heavy rainfall events have contributed to the slow, creeping movement of the overlying, joint-bounded block resulting in the progressive loading of the underlying rock mass. The rock fracture phase was extremely rapid and overlaps with the rock fall event. The kinematics of the rock fall has been interpreted from broken surfaces, scratches and positions of debris. From the timing of events, it is likely that wetting/saturation of the intact sandstone from sustained rainfall in the weeks preceding the rock fall would have significantly reduced the intact rock strength. Based on the site investigation and reconstruction of the failure mechanism, the rock fall is classified, in the Crunden and Varnes (1996) scheme, as a *complex extremely rapid rock fall and rapid dry debris slide*.

1 INTRODUCTION

This paper describes a rock fall near Pittwater that was documented in a site visit on the 24 June 2008. During an earlier site visit (9-10 January 2008) the rock fall had not been present. The rock fall represents a unique example in terms of its size, in regards to both the volume of rock debris and areal extent of the debris field, and number of volumetrically significant blocks. It was possible to document the initial position, final position and kinematics of each block, the retardation processes and also the likely groundwater hydrology and pore pressures.

The unweathered nature of the fracture surfaces on the various boulders and the very fresh appearance of debris on the bedding surface indicated that the rock fall had occurred very recently. Significant rainfall events in the week preceding the site visit would have washed clean the various surfaces.

2 SITE GEOLOGY AND GEOMORPHOLOGY

The rock fall site is located on the southern side of a small incised valley, referred to locally as Currawong. Currawong is located on the western side of Pittwater, an embayment of the southern side of the Hawkesbury River (Figure 1A). The Currawong valley comprises a small catchment (0.79 km^2) draining predominantly from an escarpment of the Hawkesbury Sandstone (Figure 1B). The edge of this escarpment is defined by a 5-15 m high cliff formed by a massive sandstone unit. The cliff encircles the valley and forms a major break in the topography. At the base of the cliff, a colluvial slope, between 100 m and 150 m wide, extends down to intersect with the floodplain/beach deposits forming the floor of the valley. The unconsolidated floodplain/beach deposits cover an area of 0.05 km^2 and consist of Quaternary fluvial sandy clay to clayey sand, inter-fingered with medium grained marine sand. The inner margins of the floodplain comprise a narrow terrace composed of matrix-supported boulder sand with larger boulders lying on and in the surface of the terrace. This terrace rises to around +3 m R.L. and is interpreted as the eroded remnant of the valley fill that would have existed during the Pleistocene high-stand. This high-stand was around 3 m to 5 m higher than current sea levels along the east coast of Australia and occurred 120,000 yrs BP (Lewis, Sloss et al. 2012).

A section through the rock fall site (Figure 2), perpendicular to the valley wall, shows the rock fall source and distribution zone as well as the morphology and interpreted geology of the colluvial slope, below the rock fall down to sea level. The location of the section is shown in Figure 1B. The source of the rock fall is the thick, massive sandstone. The bedrock immediately below the rock fall location consists of inter-bedded shale and thin (1-2 m thick) sandstone units of the Narrabeen Group. The slope below the rock fall source comprises a sequence of preferentially eroded shale units interbedded with protruding sandstone units, forming benches. These benches have been filled to capacity with colluvium comprising sandstone boulders (<1 m) in clayey sand matrix coarsening up to a medium-fine grained sand matrix, resulting in a relatively smooth slope with a maximum steepness of around 34°. There are larger sandstone boulders (1-5 m in maximum dimension) resting on and embedded within the colluvium and these are dispersed across the slope at different elevations. The colluvium on the slopes of the valley is dominated by two soil types. The upper slopes comprise medium grained sand containing boulders and pebbles of sandstone and organic material. The lower slopes (including portions of the Pleistocene terraces) consist of matrix-supported orange/brown gravelly (cobble-sized) clay with some sand (Figure 3).

A)

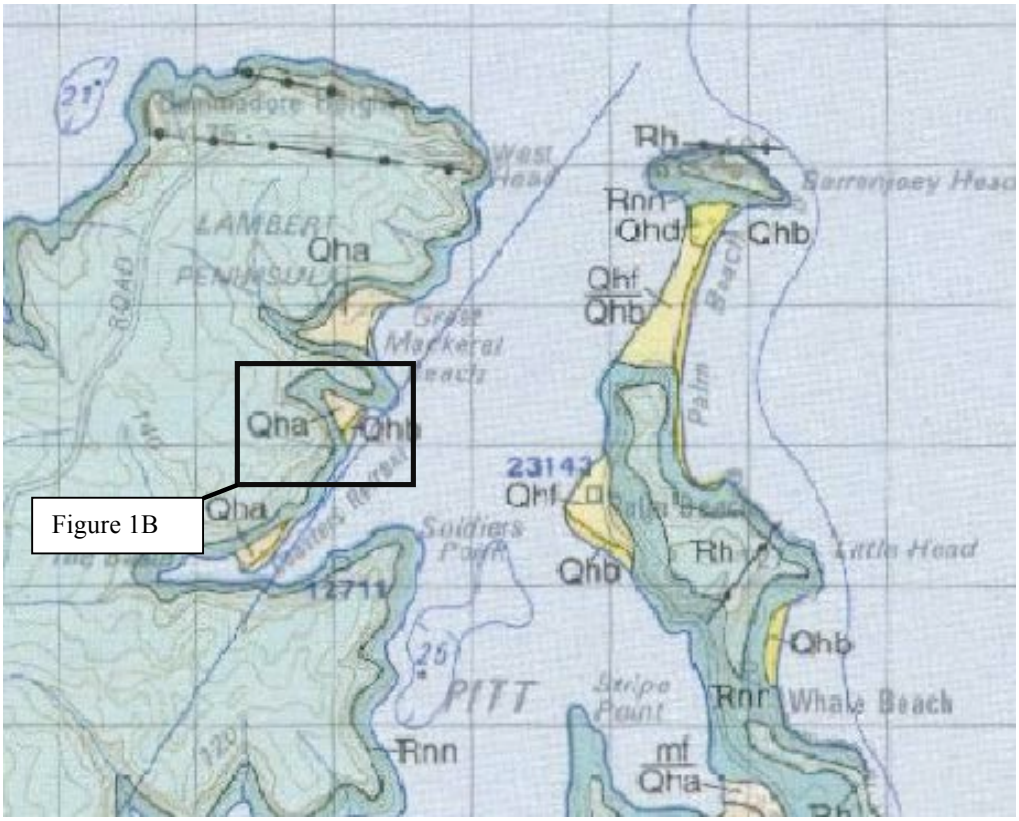

B)

Figure 1: A) Site location and surface geology , extract from (Herbert 1983) B) Aerial photograph of the local area with geological bedrock overlayed. The location of rock fall site is indicated by the red dot and the line A-A corresponds to the section shown in Figure 2.

Table 1: Bedrock Lithology at the Currawong Site (after Herbert, 1983).

Group	SYMBOL	LITHOLOGY	ENVIRONMENT
Quaternary Sediments	Qha	Silty to peaty quartz sand, silt, and clay. Ferruginous and humic in places common shell layers	Stream alluvial and estuarine sediment
	Qhb	Coarse quartz sand, varying amounts of shell fragments	Modern marine and estuarine beach
Hawkesbury Sandstone	Rh	Medium to coarse-grained quartz sandstone, very minor shale and laminate lenses	Braided alluvial channel fill
Narrabeen Group	Rnn	Interbedded, laminite, shale and quartz, to lithic quartz sandstone. Clay pellet sandstone (Garie Formation) south of the Hawkesbury River	Alluvial and deltaic

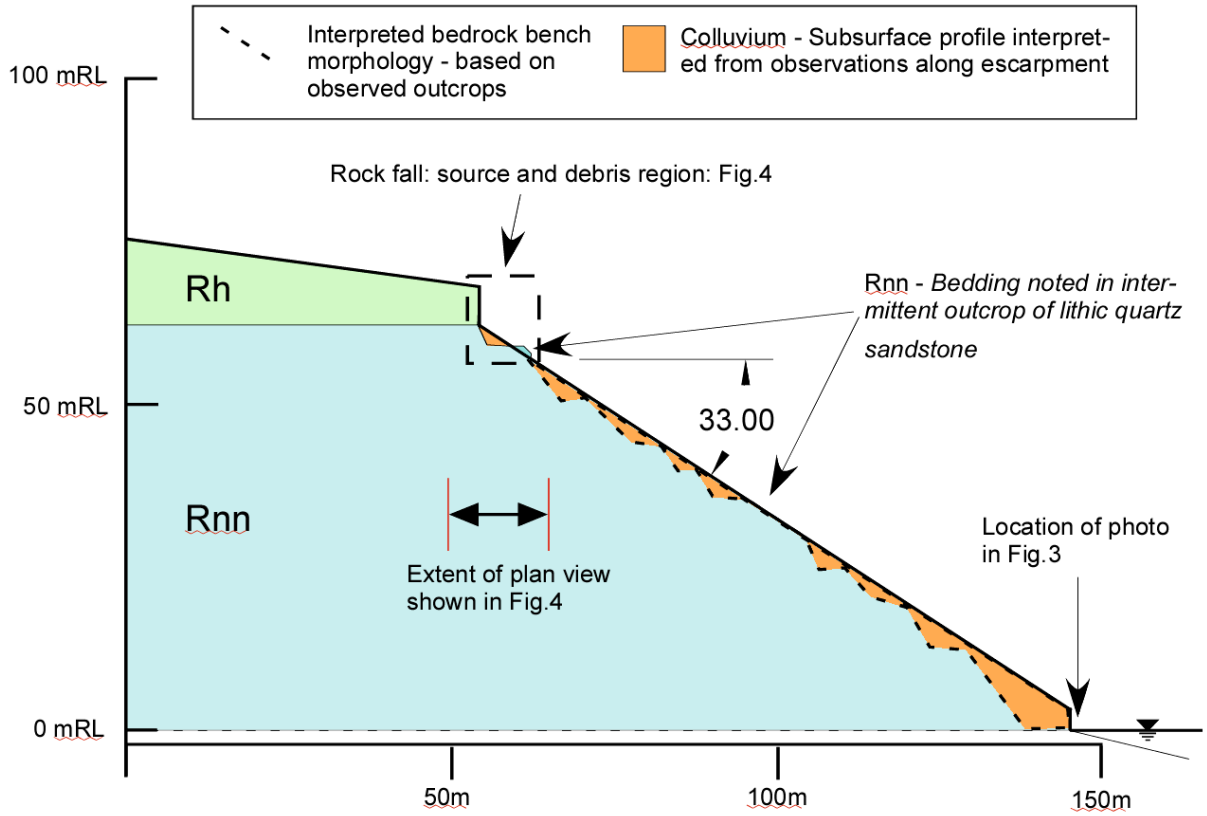

Figure 2: Cross section through valley slope at rock fall location (A-A in Figure 1).

Figure 3: Colluvium on lower slopes of valley at sea level. Site is being eroded by marine activity.

3 ROCK FALL DESCRIPTION

A plan view of the rock fall is shown in Figure 4. The extent of this plan view is shown on the sectional view in Figure 2 which aligns with the maximum slope angle direction. The dimensions of the major boulders involved in the failure are listed in Table 2. Also shown in Figure 4 and detailed in Table 2 are the travel distance vectors relating to each of the major boulders. The distance, plunge and azimuth of the centroid of each of the major blocks are detailed in the table. The travel distance vectors also coincide with the approximate direction of the steepest slope. The three major joints (J1, J2, J3) that define the pre-failure, *in situ* vertical boundaries of the 3 major boulders (B1, B2, B3) involved in the rock fall are also shown in Figure 4. The joints J2 and J3 are very significant in terms of constraining the hydrological conditions of the rockmass system discussed in Section 6.

The boulder field, the outline of which is shown in Figure 4, comprises rock fragments, (pebbles to boulders), soil and leaf matter dislodged during the rock fall event. The size of the largest boulder in the boulder field is around 0.1 m (0.001 m^3) 2 to 3 orders of magnitude smaller than the system of larger boulders that form the main volume of this rock fall. The boulder EB2 (Figure 4) was already present on the slope at the time of the failure and was impacted by boulder B3 and shunted approximately 5 m further down the slope. The furthest distance a boulder travelled from within the rock mass that failed was boulder B4, which came to rest against a tree approximately 30 m downslope from the rock fall source.

Various views of the rock fall are shown in the photographs in Figure 6 to Figure 9. Important features, discussed below, are annotated in each of the photographs and the context of each can be appreciated from the arrows (sight lines) shown on Figure 4, which indicate the vantage point from which each photo was taken.

In Figure 6, the organic root mass that filled the base of the void at the rear of the pre-rock fall position of boulder B3, is clearly visible. Also shown is a dashed orange line which marks the water/soil level prior to failure. Water seepage clearly visible on rear wall suggests water levels would have been higher during peak flow. In Figure 7, the fresh fracture surface, on the *in situ* portion of B2, indicates that the rock fall was a very recent event. The gouge mark (orange circle) on lower right of picture indicates the rear corner of failed portion of B2 rotated upwards and away from cliff face during the rock fall.

The fracture surface on *in situ* portion of B1, Figure 8, has an identical character to that of the *in situ* portion of B2. The surface defines an acute angle relative to the fracture in the block above (B2). This fracture orientation shows how the rotational movement of the rock mass away from the cliff, indicated by the gouge mark (orange circle) would have occurred. A significant gully, within the rear wall exposed by the rock fall (Figure 9), is clearly visible. Water seepage could be seen within this gully three days after the last (minor) rainfall event, suggesting that during major rainfall events, large volumes of water would have flowed through this location. The large volume of water is also indicated by the fact that the gully is filled with a substantial quantity of course debris. The wall is the remnant surface of the joint, J2 (Figure 4) that would have separated Blocks B1, B2 and B3 from the wall prior to the rock fall.

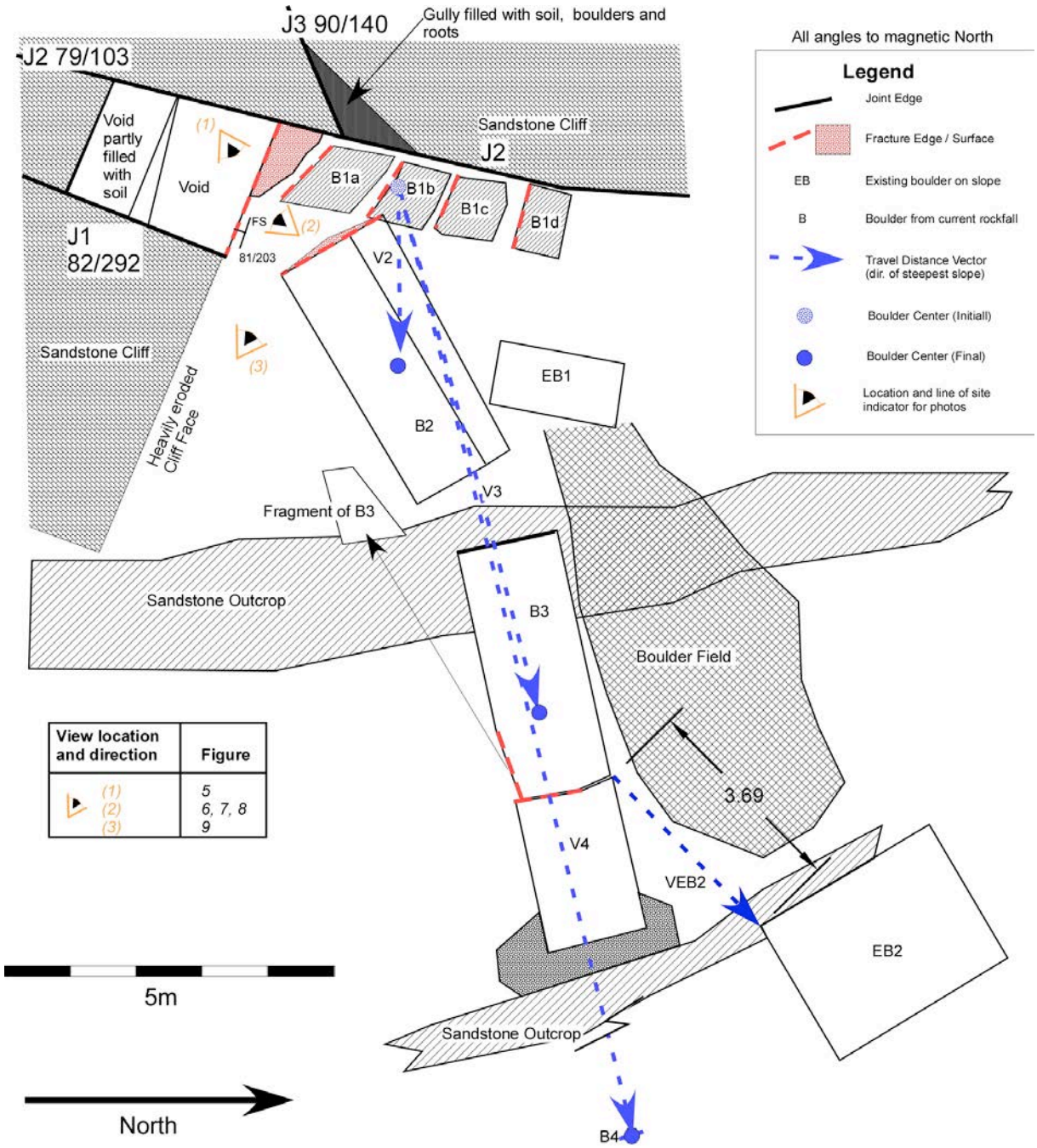

Figure 4: Plan view of rock fall, showing final position of the blocks and the interpreted original location of the block centres. Also shown are the photo locations and sandstone outcrops associated with the underlying Narrabeen Group rocks.

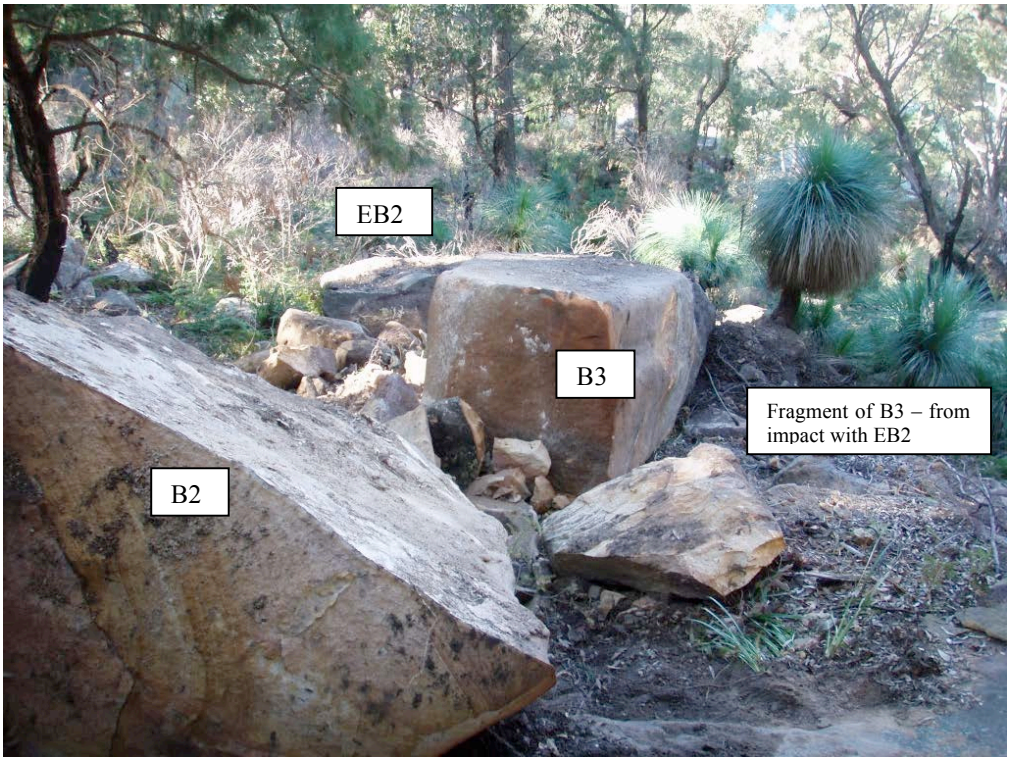

Figure 5: Extent of debris slide viewed downslope from the base of the cliff – Refer to Figure 4

Table 2: Data relating to boulders involved in rock fall (ref. Figure 4)

Block	Dimensions (m)	Volume (m^3)	Mass (t)*	Travel Distance (TD) Vector **	TD Vector length (m)	TD Vector Plunge (degrees)	TD Vector Azimuth
B1	1.0 x 1.5 x3.1	4.7	11.2	NA	NA		
B2	1.9 x 1.7 x 4.8	15.5	38.6	V2	3.7m	43	42
B3	1.6 x 1.8 x 7.4	21.3	49.6	V3	9.5m	46	56
EB1	1.9 x 1.7 x 2.3	7.5	17.8	NA	NA		
EB2	5.0 x 5.0 x 1.5	37.5	90	VEB2	4.5m	31	45
B4	0.3 x 0.3 x 0.3	0.03	0.1	V4	12.2m	35	77

* Mass calculated using density of 2.4 t/m^3, NA = Not Applicable, ** TD vectors taken as straight line between source and destination.

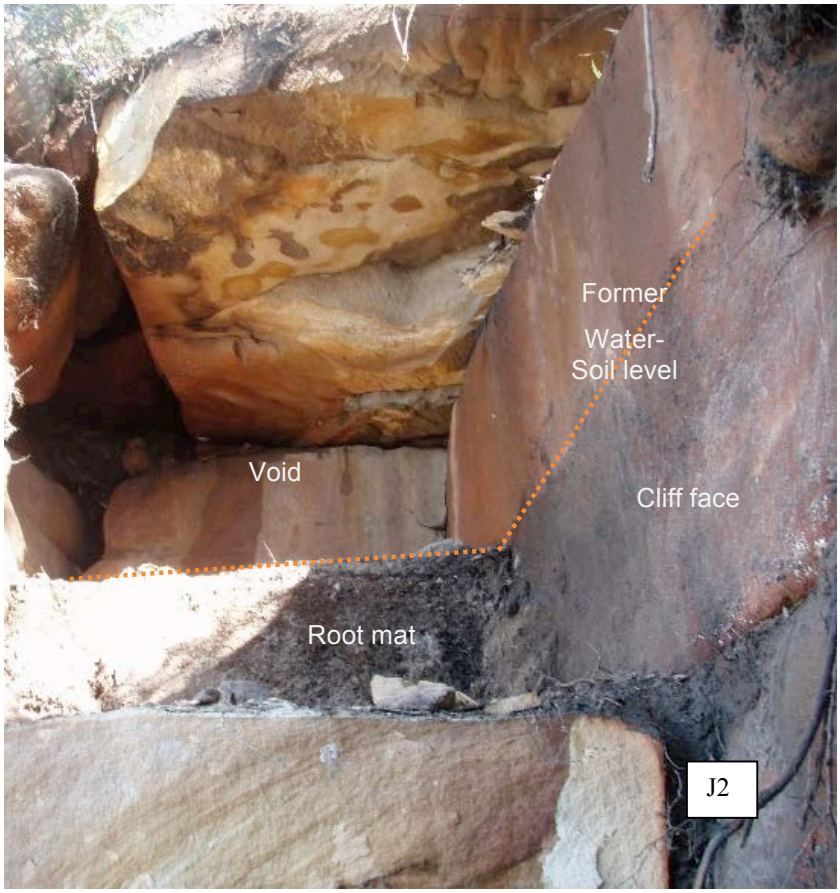

Figure 6: Photo showing open void that existed at the rear of B3 when it was *in situ*.

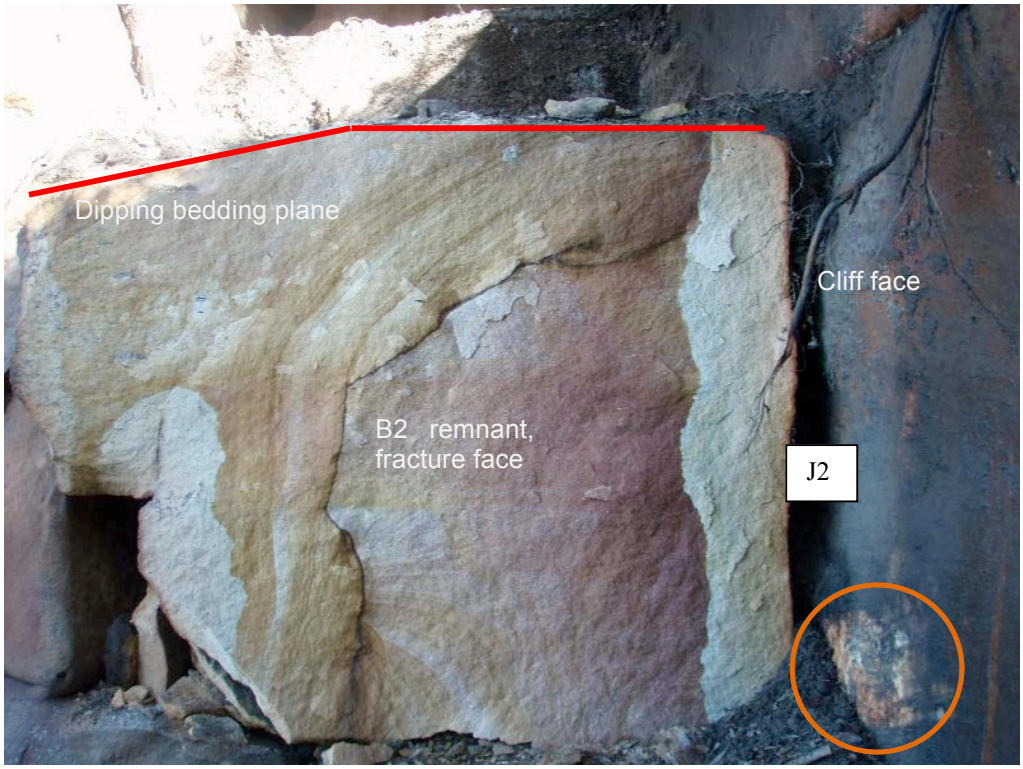

Figure 7: Fresh fracture surface on the *in situ* portion of B2.

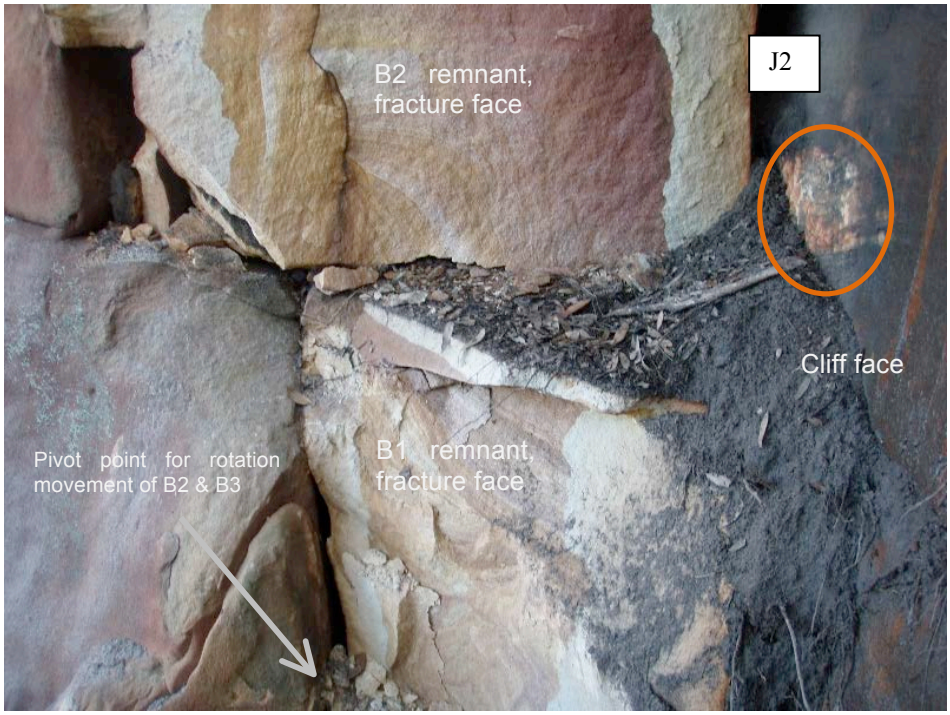

Figure 8: Fracture surface on in situ portion of B1; note acute angle relative to fracture on block (B2) above and the gouge mark (orange circle); see text for description.

Figure 9: Large gully within rear wall of cliff, exposing one surface of the Joint, J2 (Figure 4).

4 CONSTRAINTS ON ROCK FALL TIMING

It is certain that the rock fall event occurred sometime between the two site visits on the 9th of January and 24th of June. Measured rainfalls at Palm Beach, on the other side of the Pittwater from Currawong, are shown in Figure 10. A key factor in determining a more precise timing of the event is that although there had been extensive rainfall in the area in the 5 months between the two site visits, none of the impact marks, gouges or fracture surfaces had been washed clean

of the crush debris. Also, soil on the newly exposed surfaces of previously closed joints had not yet been washed off. This indicates that the rock fall occurred sometime after the last significant rainfall event of around 100 mm at the beginning of July. Below are listed the observations that indicate a possible failure mechanism

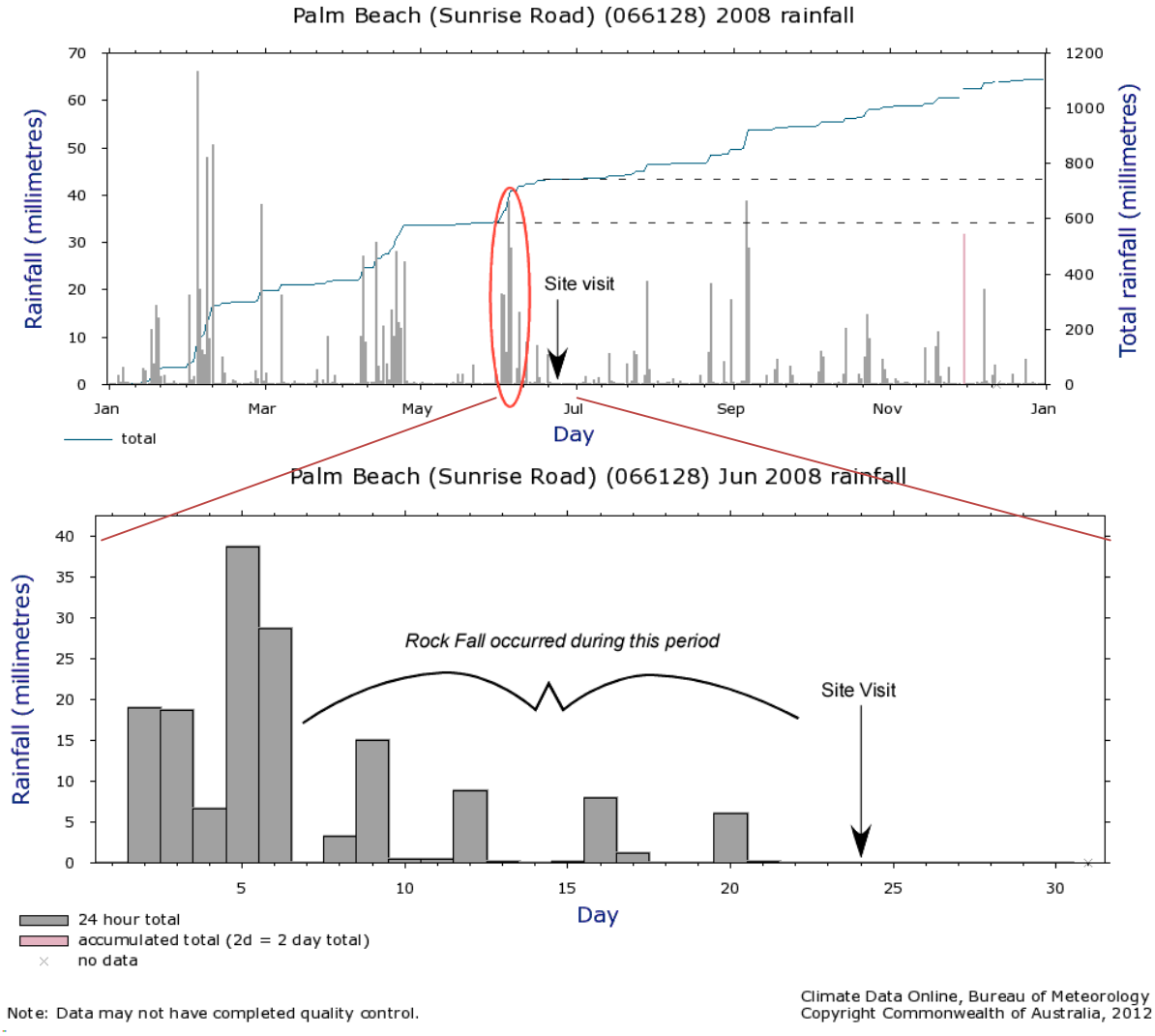

Figure 10: Rainfall events in early June, 2008, prior to site visit.

5 MECHANISMS CONTRIBUTING TO THE ROCK MOVEMENT

The overall rock movement process is inferred to have occurred in three distinct phases; an initial creep-loading phase, a progressive but extremely rapid rock fracture phase, and the ultimate rock fall phase, which overlapped with the rock fracture phase. These movement phases have been reconstructed from a number of post-failure observations and the reconstructed pre-failure positions of the rock fall boulders. The travel distance of all the major boulders has been recorded and a reconstruction of the failure process has been performed on the basis of the boulder orientations and scratch marks on a number of surfaces. Although substantial kinetic energy would have been developed in the larger blocks, the roughness of the underlying slope and impacts with blocks already present on the slope (EB1 & EB2) has significantly retarded the run out of the debris. It can be seen from the orientation of the boulder field, the location of blocks EB1 & EB2 and the final positions of B2 and B1 (Figure 4), that although the blocks followed the steepest path trajectories, the direction of movement was significantly altered during the rock fall event.

A cross section along the centre line of the remnant failed cliff is shown Figure 11A and a section across the failed surfaces is shown in Figure 11B. The locations of these sections within the rock fall site are shown in the insert in the figure. The original and pre-rock fall positions of B3, shown by the grey and black dashed lines in Figure 11A respectively, have been interpreted from the fact that the void, which has become partially filled with soil and roots, is not a feature of the rock forming process. The pre-failure location of blocks B1, B2 and B3 is reconstructed from measured dimensions of the blocks and a visual correlation between the new and old fracture surfaces. The soil- and

root-filled void behind B3 suggests the block had been migrating progressively out of its original location, in a direction parallel to the cliff line, prior to the ultimate rock fall.

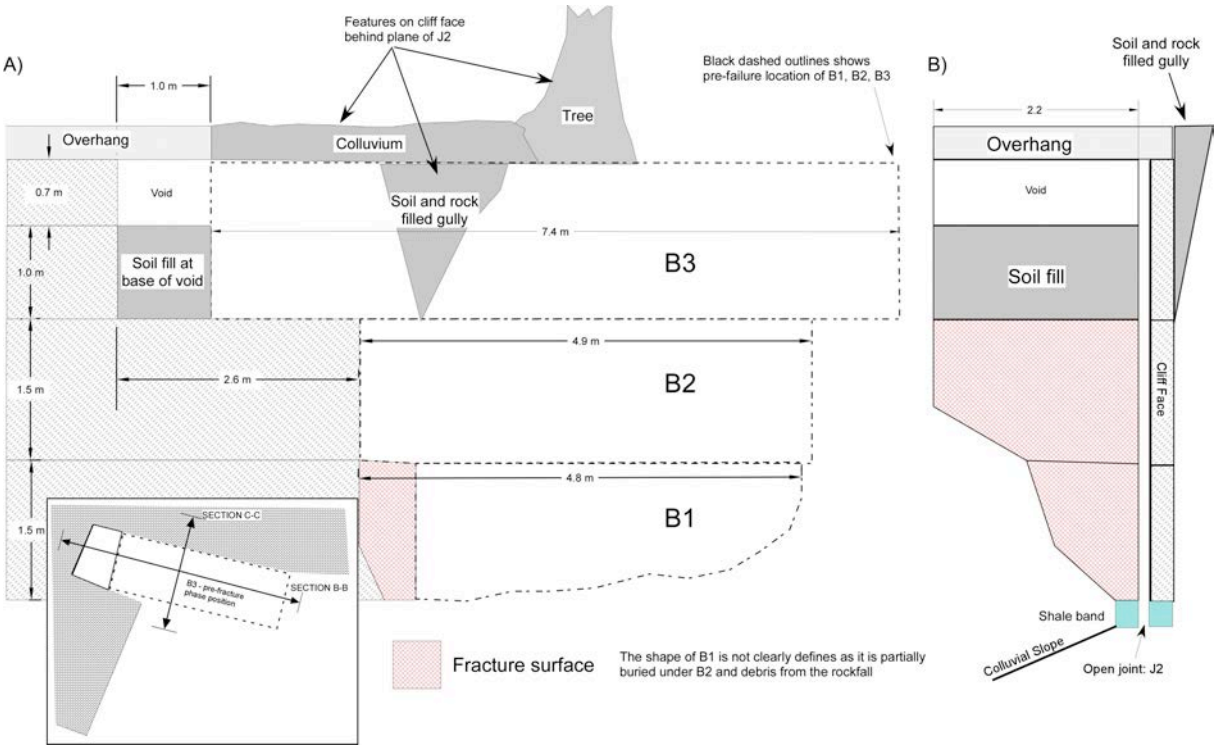

Figure 11: Sections through remnant failed rock mass A) Section B-B, parallel to cliff face and B) Section C-C, perpendicular to cliff face.

5.1 CREEP-LOADING PHASE

The following evidence suggests a movement mechanism for B3:

- B3 was originally bounded on all sides by pre-existing joint and bedding surfaces,
- block shape compatibility indicates that B3 had originally occupied the space of the void,
- the presence of a well consolidated soil mass with tree roots (Figure 6) indicated that the void has opened gradually by a creeping movement of B3, well before the rock fall occurred,
- the soil and boulder filled gully in the face behind B3 provided an opportunity for porous material with delayed drainage to hold water for brief periods during heavy rainfall, and also an access point for tree roots to intrude between B3 and the face (Figure 9),
- water marks on the wall in which the gully is located indicated that water levels could have been maintained 0.5m above the floor of the void (Figure 6), at least during heavy rainfall,
- large tree roots were exposed on the wall which would have been the joint (J1-J2, Figure 4) between blocks B1,B2,B3 prior to the failure (Figure 9),
- B3 had been stable through the proceeding 4 significant rain events since the 9th January rain event.

The incremental movement direction of Block B3 prior to the rock fall was predominantly parallel to the cliff face (i.e. to open the void). This is interpreted from the fact that the root mat filling the void behind B3 has a vertical margin that is perpendicular to the cliff face (Figure 6 and Figure 11). The texture of the root mat indicates that it would have been in full contact with B3 prior to the failure, meaning that J2 (Figure 6) would have been essentially closed. The upper surface of block B2, which B3 was initially resting on, is partly dipping outwards from the cliff face (Figure 7), encouraging sliding and lowering the available frictional resistance.

The incremental movement of B3 is most likely to have been initially driven by intermittent water pressure build up in the debris-filled gully and in the vertical open joint (J2, Figure 6, Figure 11) between B1, B2 and B3 and the sandstone cliff. The role of water in driving creep processes in rock masses in not straightforward. It is postulated that the build-up

of water pressure in a joint would require some kind of "crack-seal" phenomenon involving debris from the gully impeding water flow through the joint system behind the failed rock mass, so that some height of excess water could be maintained. Immediately after a small block movement, the "seal" would be broken and surface water flow concentrated in the gully would again flow out freely through the joints. Over a period of rainfall events, fine grained sediment would again accumulate and progressively fill the new space. Once flow had again been restricted, excess water pressure would develop during high rainfall events, resulting in another incremental movement of B3.

While water is a plausible and likely major agent in the movement it is also likely that generations of opportunistic tree roots have contributed to the creep of B3: indirectly, by trapping soil, and directly, by applying pressure to blocks.

5.2 ROCK FRACTURE AND ROCK FALL PHASES

The significant areas of freshly fractured rock in B1 and B2 suggest that failure involved more than just toppling, due to a simple rearrangement of blocks through creep to attain an unstable arrangement. The presence of fresh fracture surfaces on the blocks beneath B3 suggests that failure of the rock itself contributed to this rock fall.

The largest components of debris within the boulder field (Figure 4) are around 3 orders of magnitude smaller than the main boulders within the rock fall. Consequently, it is assumed that they are not likely to have contributed significantly to the kinematics of the rock fall. A sequence of events associated with the rock fall has been reconstructed from (1) the observed gouge marks on the cliff face (Figure 7, Figure 8, Figure 9), (2) impact marks and movement directions of existing blocks on the slope (EB1 and EB2) and (3) the final position of the blocks (Figure 4). These are:

- The incremental movement of B3 would have been progressively modifying loading conditions of the underlying blocks, B2 and B1 (Figure 11).
- B1 is likely to have yielded first, probably by splitting due to the load from B2 producing direct and/or indirect tension within it.
- Failure of B1 would cause changes in the support conditions for B2, exacerbating the tension in it, causing it to fail by splitting also.
- Fragments of B2 and B3 rotated downwards and out from the cliff face.
- The motion of B2 was arrested by an impact with EB1.
- Having lost support, B3 tobogganed off B2.
- Orientation of boulder field shows initial movement vector of B3 prior to impact with EB1.
- B3 impacted EB2, and landed on slope, resulting in the fragmentation of B3 (Figure 4). Associated debris either cascaded from the blocks as they moved (i.e. rocks within the debris field, Figure 4) or was ploughed forward by the falling blocks.
- EB2 was pushed into its final position by the impact of B3.

The orientation of the fracture surface between B1a and the remnant cliff (Figure 4, acute rather than parallel) is likely to be a result of the eroded morphology of the underlying shale band that had been supporting B1 (Figure 11B). The void under B1 is the result of undercutting erosion into the underlying shale band. This would have occurred preferentially from the outer edges, inwards. This would result in decreased support and stress concentration over time, for the overlying blocks, B1, B2, and B3. The morphology of this under cutting erosion would also have contributed to creep in the overlying rock mass and the outward rotation of B1, away from the cliff face, after the rock mass failed.

The mode of failure of B1 and B2 is interpreted as being a "cantilever failure" (Selby 1993). In this type of failure, locally varying support of overhanging blocks produces tensile stresses that are concentrated in the upper portion of the block, while below a neutral axis through the central portion of the block compressive stresses occur. The rock is most likely to fail in tension as the tensile strength is typically much lower than the compressive strength (Brady and Brown 2005). Tensile strength is, however, extremely sensitive to pre-existing defects within the intact rock mass. There is clear evidence in this study that the rock in each fracture surface is not completely uniform, with evidence of some pre-existing fractures, and the strength is therefore likely to have been lower than any intact strength (Figure 7 and Figure 8).

Based on the site investigation and the reconstruction of the failure mechanism described above, the rock fall is classified as a *complex extremely rapid wet rock fall and rapid dry debris slide*, according to the Cruden and Varnes (1996).

5.3 ROLE OF WATER

The role of water in the failure process can be deduced from the rainfall record for the site region, Figure 10, and a number of observations at the rock fall, including;

- Dripping water along J2 (Figure 9) from bedding planes and base of gully (Figure 8),
- Residual dampness over cliff face (Figure 9) and around the gully,
- Intensive orange staining and flow weathering over cliff face around gully with sharp boundary to lichen covered grey sandstone away from gully (Figure 9),
- Large boulders in sand-clay matrix and concentrated root growth filling a gully, with thick colluvium and a ground surface higher than the upper surface of B3, prior to failure (Figure 11),
- Fresh rock exposed in *in situ* fractured boulders.

A mechanism for incremental block movements driven by heavy rainfall was described in the previous section, which invoked the involvement of soil and roots in filling cracks sufficiently to delay the escape of water and sustain a water pressure thrust on the faces of the block. The obvious role of rainfall in this is to be heavy enough to produce infiltration which exceeds the transmissive capacity of the debris-filled joints. Clearly, this is most likely to happen during the most intense of rainfall events.

A less obvious role of rainfall is to have been sustained enough, so as to saturate the ground sufficiently to maximise the generation of runoff (flowing surface water). This suggests that the total amount of rain may be as important as the rainfall intensity.

This idea is supported by the evidence of fresh small debris still on exposed surfaces, that the rock fall did not occur during the many heavy rainfall events prior to the 9th of June. Rather, it seems to have occurred after all of them, suggesting that sustained and comprehensive wetting of the ground was a key factor, and that only after the ground was thoroughly wet, could the rock fall occur. Given the large amount of rain that fell in the weeks before, it could also be suggested that thorough wetting is a slow process requiring sustained rainfall over an extended period. Little more can be concluded about the actual event that triggered the slide without temporal rainfall intensity graphs for the individual rainfall events.

However, from a further consideration of the possible effects of saturation, it is not necessary that the rock fall should even coincide with a particular rainfall event. The timing of this particular event suggests that another factor that may have played a significant role in this rock fall is the strength reduction effect that water has on rocks, particularly cemented sedimentary rocks. Wet/dry strength variation is a well-recognised phenomenon in geo-materials(Hawkins and McConnell 1992), with Vásárhelyi (2003) reporting that for sandstones, the strength reduction is commonly around 20%. Pells (2004) provides data to show that for Hawkesbury Sandstone, the saturated compressive strength may be less than 40% of the fully dry strength, and Gunsallus and Kulhawy (1984) suggests that similar behaviour is valid for tensile strength. The key role played by tensile failure in this rock fall, and the delay between the most of the rainfall and failure, suggests that wetting-induced strength reduction is likely to have been an important factor in triggering the event.

6 TRAVEL DISTANCE

Estimation of risk to persons and property due to rock fall typically requires estimation of travel distance. Finlay *et al.* (1999) presents a summary of travel distance versus landslides volume for a large number of landslides including rock falls. The summary chart from Finlay *et al*. has been reproduced below, with the travel distance for the rock fall documented in this paper plotted on the chart for comparison purposes. The travel distance for a block of volume V is presented in terms of the variable F, defined as the height (H) divided by the runout distance (L). The height of the Currawong rock fall has been taken as 5.6 m and the runout distance between 9.5 m and 12.2 m. As can be seen, a 21 m^3 rock at Currawong has travelled a distance within the range of that documented in Finlay *et al*. (1999) but towards the larger run out distance.

Finlay *et al*. (1999) also presents an equation for estimating travel distance for rock falls based on multiple regression analysis of travel distance data for a large number of case studies. Finlay *et al.* states that the regression is mostly applicable to the situation where the debris runs out onto a near horizontal slope below. At Currawong this runout slope is approximately 33^o. Applying the Finlay et al equation to the Currawong rock fall results in an estimated travel distance of between 0.5 m and 8.2 m. This is approximately half the travel distance observed. The longer travel distance can be explained by the steeper slope below the face.

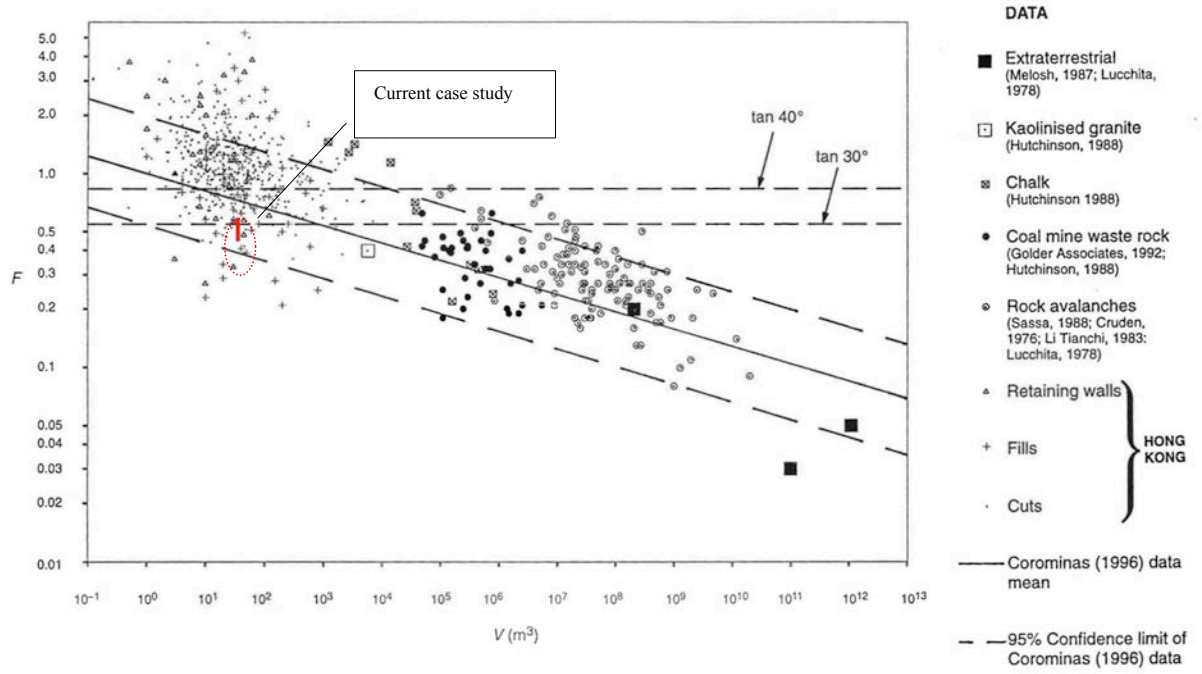

Figure 12: Plot of LogF versus logV for various landslides (from Finlay, Mostyn *et al*.(1999)

7 CONCLUSION

The case history presented herein represents a detailed record of a rock fall in the Hawkesbury Sandstone, within the Currawong valley on the western side of Pittwater.

An initial phase of movement in the form of creep movement of an overlying rock block was driven by high transient water pressures, cracking and sealing of the opening joint during rainfall events and increasing root pressure. This creep movement resulted in a gradual increase in the load distributions concentrated in the underlying blocks. The rock fall event itself was initiated by the second phase of movement, the rapid cantilever failure of overloaded intact Hawkesbury Sandstone, with reduced strength resulting from its progressive saturation from sustained rainfall in the weeks before. Based on the site investigation and reconstruction of the failure mechanism the rock fall is classified as a *complex extremely rapid wet rock fall and rapid dry debris slide*, according to Cruden and Varnes (1996).

In this regard, the paper represents a unique and valuable record. Both the initial phases of rock movement were able to be recorded as well as the kinematics of all the major rock blocks within the fall. The understanding of rock fall process and the identification of future potential failures within the Sydney Basin would be greatly improved by more of this type of data.

8 ACKNOWLEDGEMENTS

The field mapping that this paper is derived from was undertaken by the Author in 2008 while working for Pells Sullivan Meynink. The authors would like thank PSM for the permission to publish this data.

9 REFERENCES

Brady, B. H. G. and E. T. Brown (2005). Rock Mechanics for underground mining. New York, Kluwer Acedemic Publishers.

Cruden, D. M. and D. J. Varnes (1996). Landslide Types and Processes. Landslides: investigation and mitigation. A. K. Turner and R. L. Schuster, Transportation Research Board. **247**.

Finlay, P. J., G. R. Mostyn, *et al*. (1999). Landslides: Prediction of Travel Distance and Guidelines for vulnerability of Persons. 8th Australian New Zealand Conference on Geomechanics. Hobart, Australian Geomechanics Society. **2:** 105-113.

Gunsallus, K. L. and F. H. Kulhawy (1984). "A comparative evaluation of rock strength measures." International Journal of Rock Mechanics and Mining Sciences & Geomechanics Abstracts **21**(5): 233-248.

Hawkins, A. B. and B. J. McConnell (1992). "Sensitivity of sandstone strength and deformability to changes in moisture content." Quarterly Journal of Engineering Geology and Hydrogeology **25**(2): 115-130.

Herbert, C. (1983). Sydney 9130. 1:100 000 Geological Sheet Sydney, Geological Survey of New South Wales.

Lewis, S. E., C. R. Sloss, *et al*. (2012). "Post-glacial sea-level changes around the Australian margin: a review." Quaternary Science Reviews(0).

Selby, M. J. (1993). Hillslope materials and processes. Oxford, Oxford university Press.

Vasarhelyi, B. (2003). "Some observations regarding the strength and deformability of sandstones in case of dry and saturated conditions." Bulletin of Engineering Geology and the Environment **62**(3): 245-249.